



Development of 3D SiC radiation detector

Hongwei Liang¹, Xiaochuan Xia¹, Zhenzhong Zhang¹, Ruiliang Xu¹

Xin Shi², RuiRui Fan³, Xinbo Zou⁴

¹ *Dalian University of Technology*

² *Institute of High Energy Physics Chinese Academy of Sciences*

³ *Spallation Neutron Source Science Center*

⁴ *School of Information Science and Technology*

22-6-2022



Outline

- Motivation
- Fabrication of 3D SiC radiation detector
- Characteristics of 3D SiC radiation detector
- Prospect

Advantages of semiconductor radiation detectors

**Narrow band gap
semiconductor detector
w~3eV**

Fano factor (~0.1)

- ✓ Energy resolution
- ✓ Detection efficiency
- ✓ Pulse rise time
- ✓ Energy linear range
- ✓ Integrated
- ✗ Small size
- ✗ Radiation damage
- ✗ High temperature
- ✗ Protect from light

**Gas detector
w~30eV**

Fano factor (0.2~0.5)

- ✓ Energy resolution
- ✗ Detection efficiency

**Scintillator detector
w~300eV**

Fano factor (~1)

- ✓ Detection efficiency
- ✗ Energy resolution
- ✗ Carrier collection

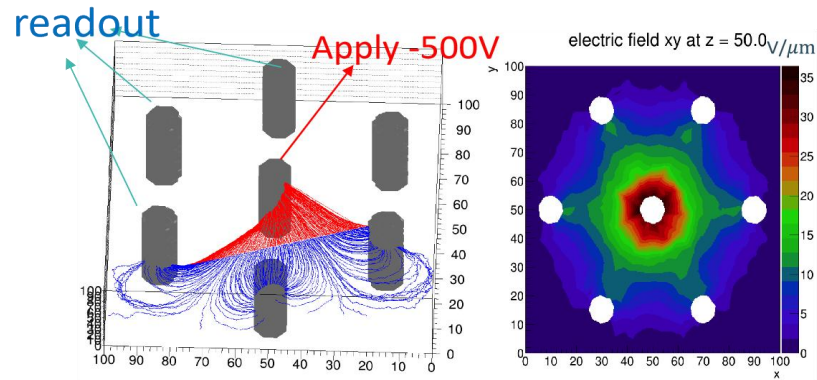
Wide bandgap semiconductor based detector
can meet the demand

Motivation for the development of 3D SiC radiation detector

1. Wide band gap (3.2 eV), High breakdown field strength, Mature process technology
2. Narrow electrode spacing – good time resolution and charge collection
3. Good singlecrystal quality – Thick thickness – larger charge collection and signal
4. More radiation resistant than 2D SiC

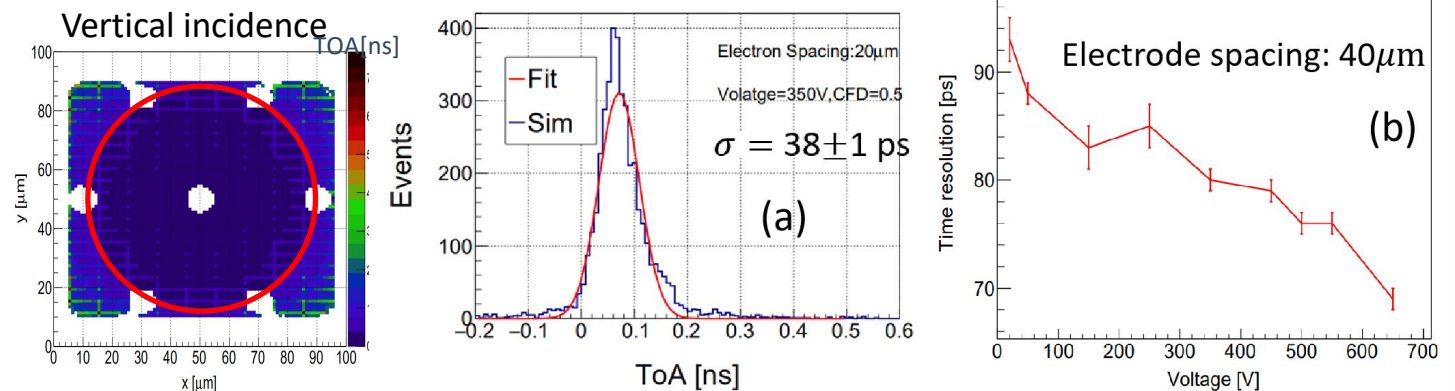
3D-SiC simulation – time resolution:

Device structure



- **SiC structure.** Electrode radius $5 \mu\text{m}$, electrode spacing $40 \mu\text{m}$ and $100 \mu\text{m}$ thick
- **Drift path:** blue electrons and red holes in Fig.a
- **Electric field xy plane at $z = 50 \mu\text{m}$** in Fig.b

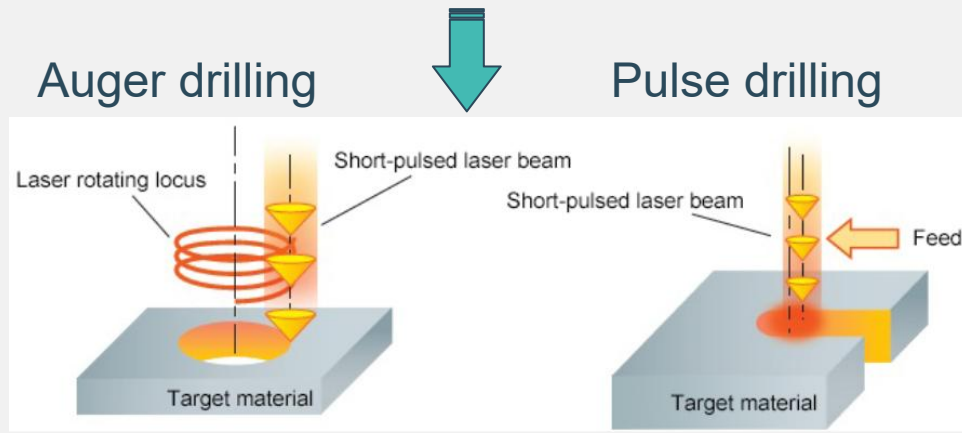
Device performance



- **Detector scan:** 10000 events. Step: $1 \mu\text{m} \times 1 \mu\text{m}$
- **Fig.a:** Time resolution is 38 ps at 350V with electrode spacing $20 \mu\text{m}$
- **Fig.b:** Time resolution vs voltage

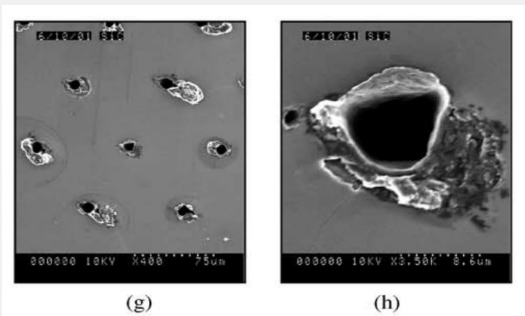
Method of making 3D structure

1. ICP etching (Inductive Coupled Plasma Emission Spectrometer Etch)
2. Chemical or electrochemical etching
3. Laser drilling



Advantage of laser drilling technology

1. Suitable for a variety of materials
2. Few steps and parameters
3. Short process time



Giulio Pellegrini and P. Roy *et al.*, "Technology development of 3D detectors for high-energy physics and imaging" Nuclear Instruments and Methods in Physics Research A 487 (2002) 19–26.

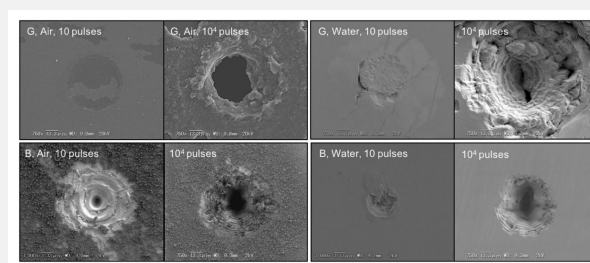
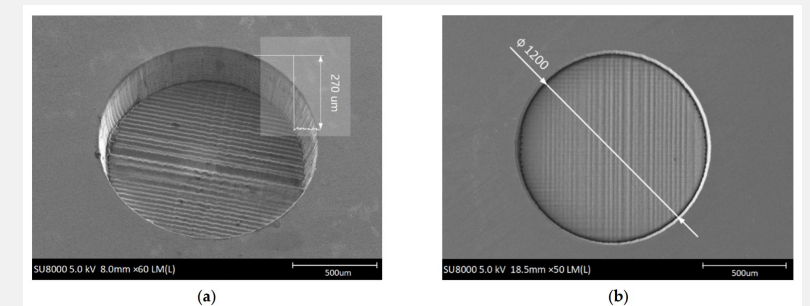


Fig. 2 SEM images of top view of drilled centers with $F = 60 \text{ J/cm}^2$ of 1064 nm irradiance. In each figure, characters "G" and "B" stand for Gaussian and Bessel beams, respectively. In the case of Bessel beam irradiation, entrance of the hole enlarged with increasing pulse numbers affected by side lobes heating. Gaussian irradiation under water environment led to formation of cracks

Byunggi Kim and Ryoichi Iida *et al.*, "Mechanism of nanosecond laser drilling process of 4H-SiC for through substrate vias" Appl. Phys. A (2017) 123:392.



Lukang Wang and You Zhao *et al.*, "Design and Fabrication of Bulk Micromachined 4H-SiC Piezoresistive Pressure Chips Based on Femtosecond Laser Technology" Micromachines 2021, 12, 56.

Process flow of making 3D SiC structure

Semi-insulating SiC
single crystal
350 μm thickness

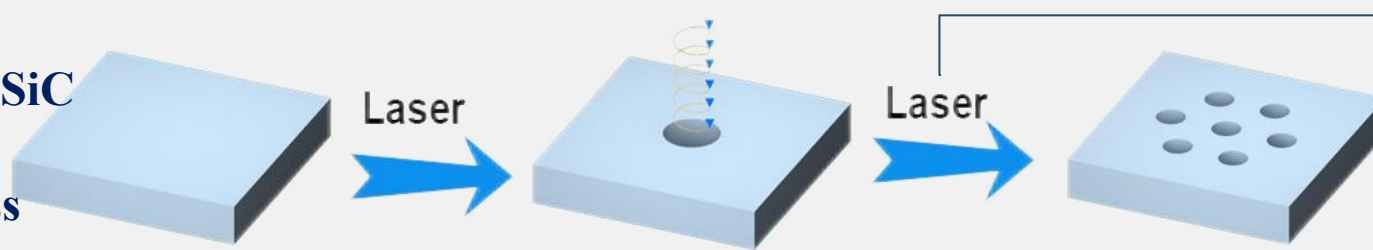


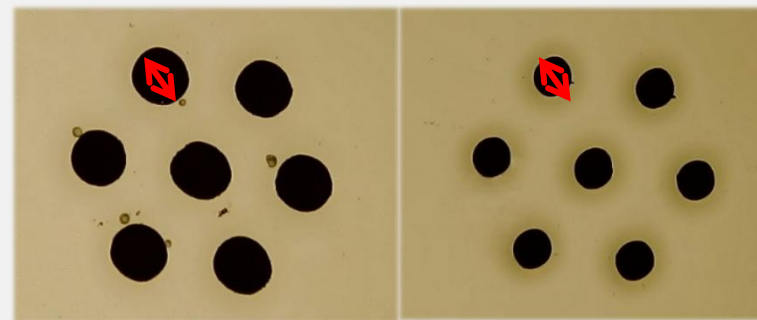
Figure 1 Laser drilling preparation process

Table 1 Laser processing parameters

Device model	FM-UVPM3A
Laser wavelength	355nm
Processing power	3W
Pulse Width	12ps
Processing speed	100mm/s
Processing time	30min/pcs

Table 2 Diameter of the cylinder at the top and bottom of the sample

Hole	Diameter (μm)
Entrance	103
Exit	81

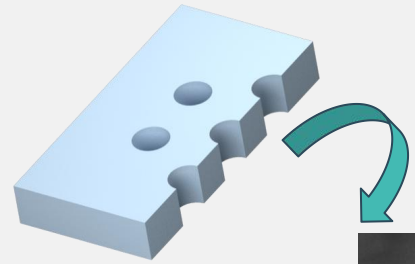


Entrance hole / Exit hole

The taper of the through hole
could be calculated as:

$$(103-81) / 362 \approx 1/16$$

Morphology and composition of through hole



Scanning electron microscope (SEM) image

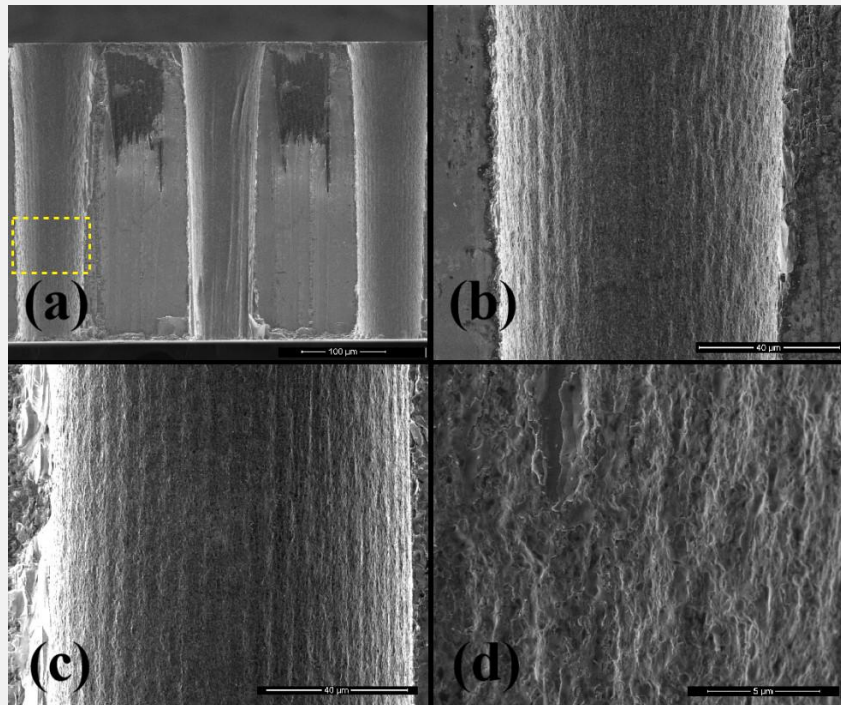


Fig. 2 SEM cross-sectional images of laser-drilled through holes in SiC (a) overall and (b)-(d) partial enlarge morphology

Energy dispersive X-ray spectrometry (EDS) image

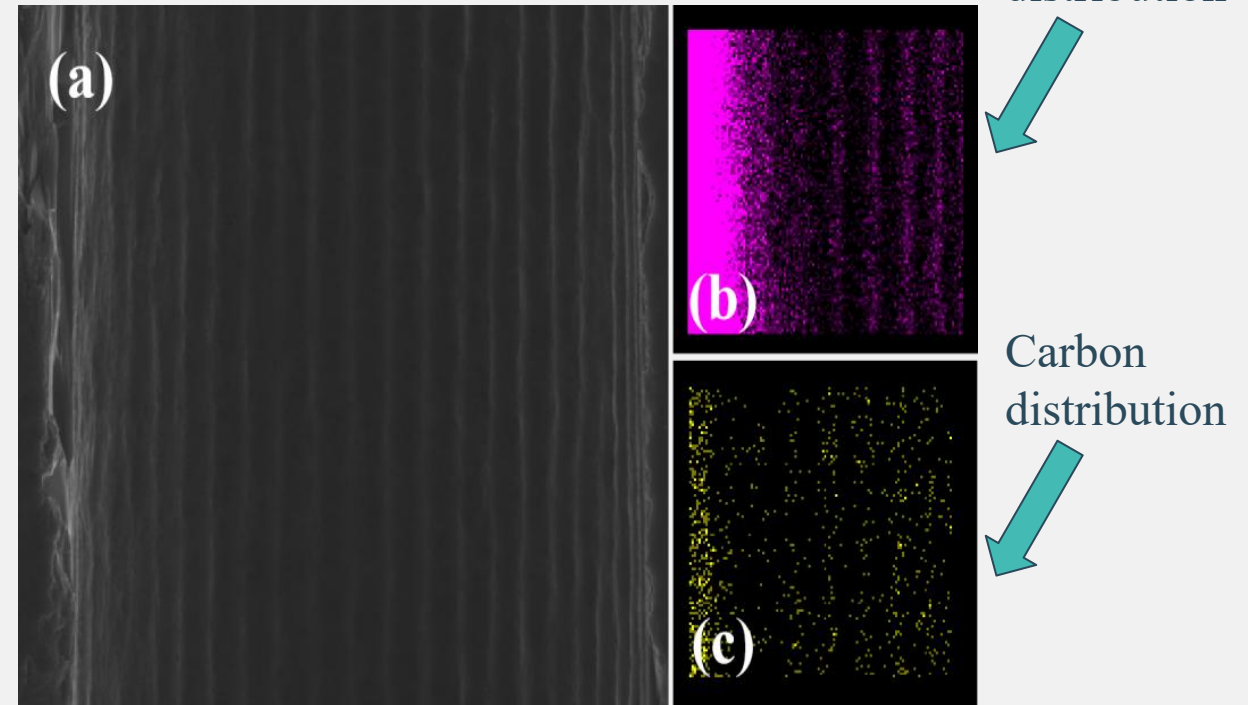


Fig. 3 EDS mapping of silicon and carbon element, (a) the selected area morphology, (b) distribution of silicon element, (c) distribution of carbon element

Crystal quality of the through hole after laser drilling

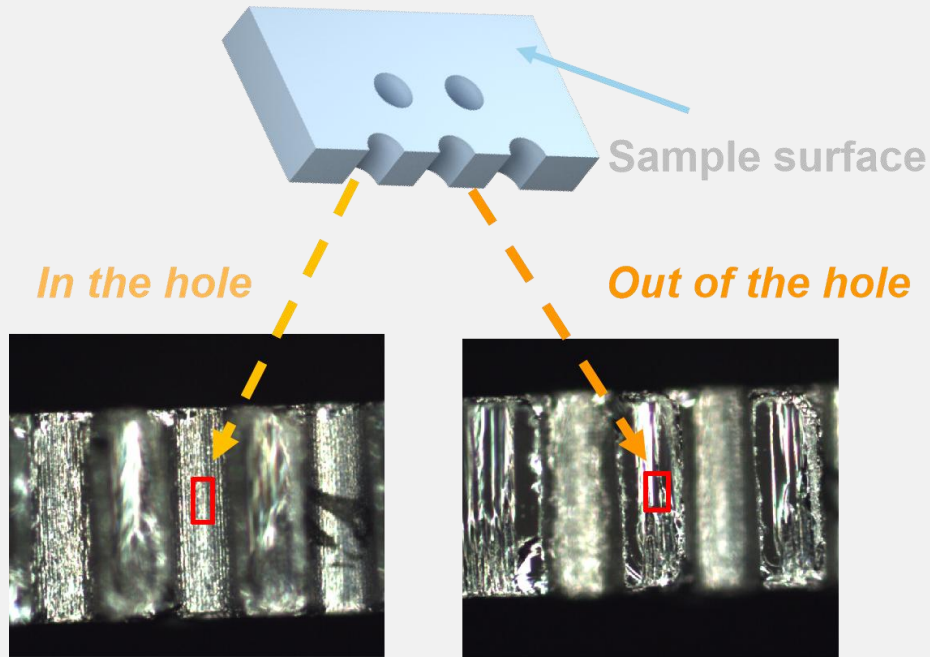


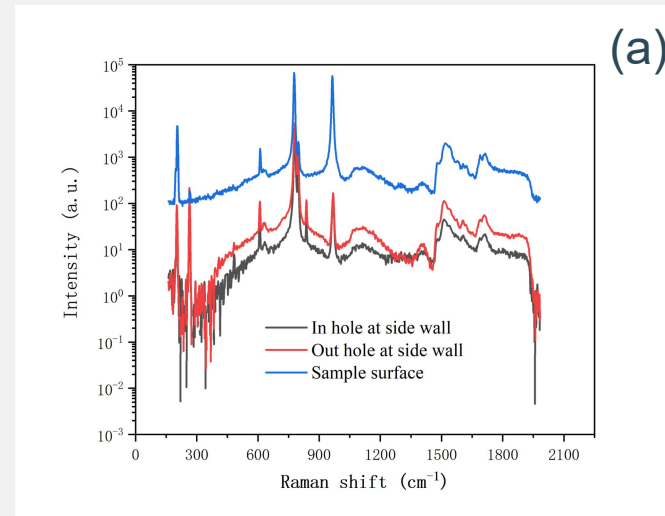
Fig.4 Schematic of Raman test area

Undoped 4H parallel		Undoped 4H perpendicular	
Peak	Slope (cm ⁻¹ /K)	Peak	Slope (cm ⁻¹ /K)
207.2	-0.0034	268.1	-7.45E-4
268.1	-0.0018	612.2	-0.0056
612.5	-0.0086	785.4	-0.0157
797.4	-0.0164	800.3	-0.0144
799.4	-0.0164	840.9	-0.0131
968.3	-0.0182	974.6	-0.0157

J. Raman Spectrosc. **2009**, *40*, 1867–1874

Table 3 Raman peak positions of 4H SiC

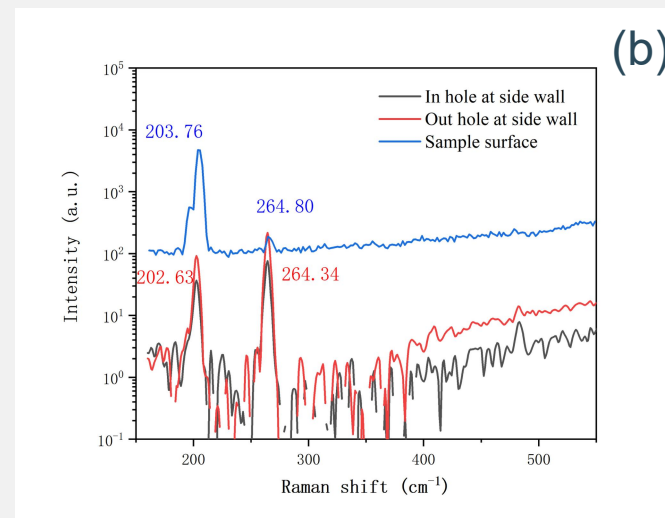
Raman measurement



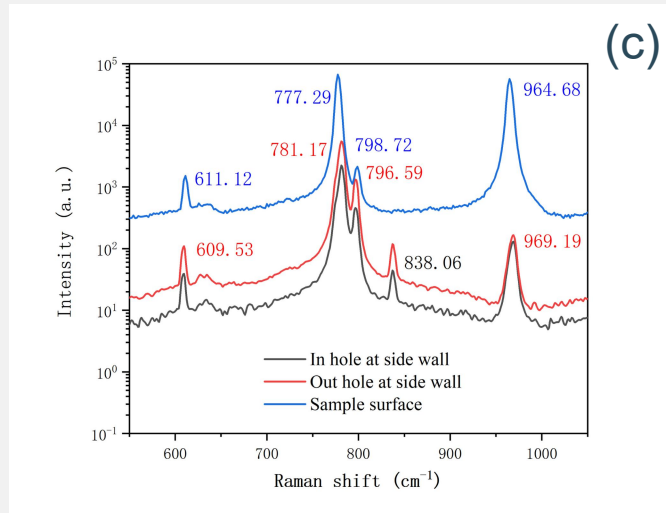
(a)

Fig. 5 the micro Raman results obtained in/out of the hole, as well as on the sample surface (a) full spectrum (b) and (c) local magnification

It shows that SiC sensitive region maintains high crystal quality after laser drilling.



(b)



(c)

Process flow of making 3D SiC structure

Fig. 6 Process of indium filling

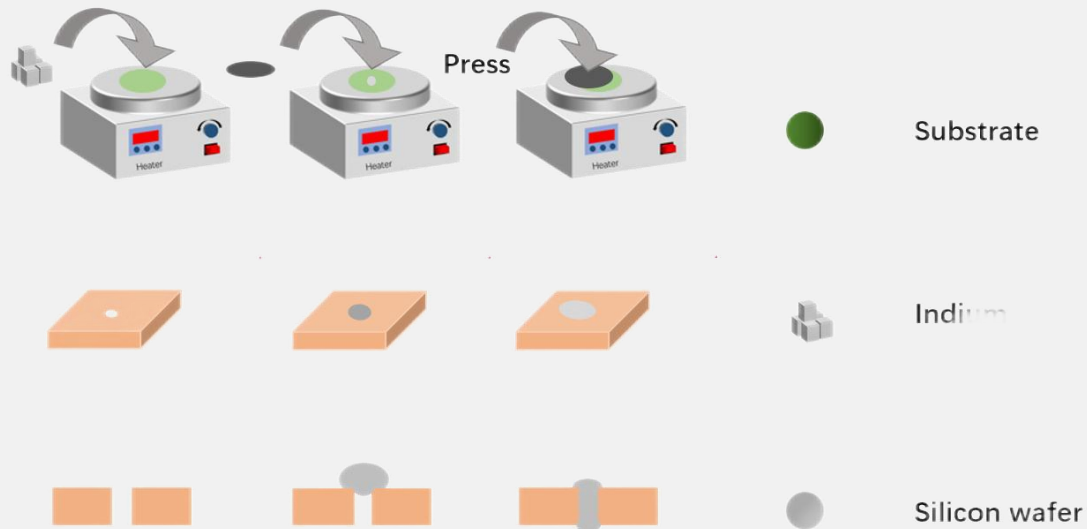
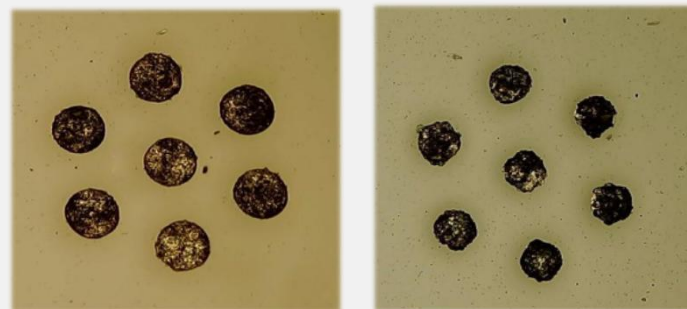
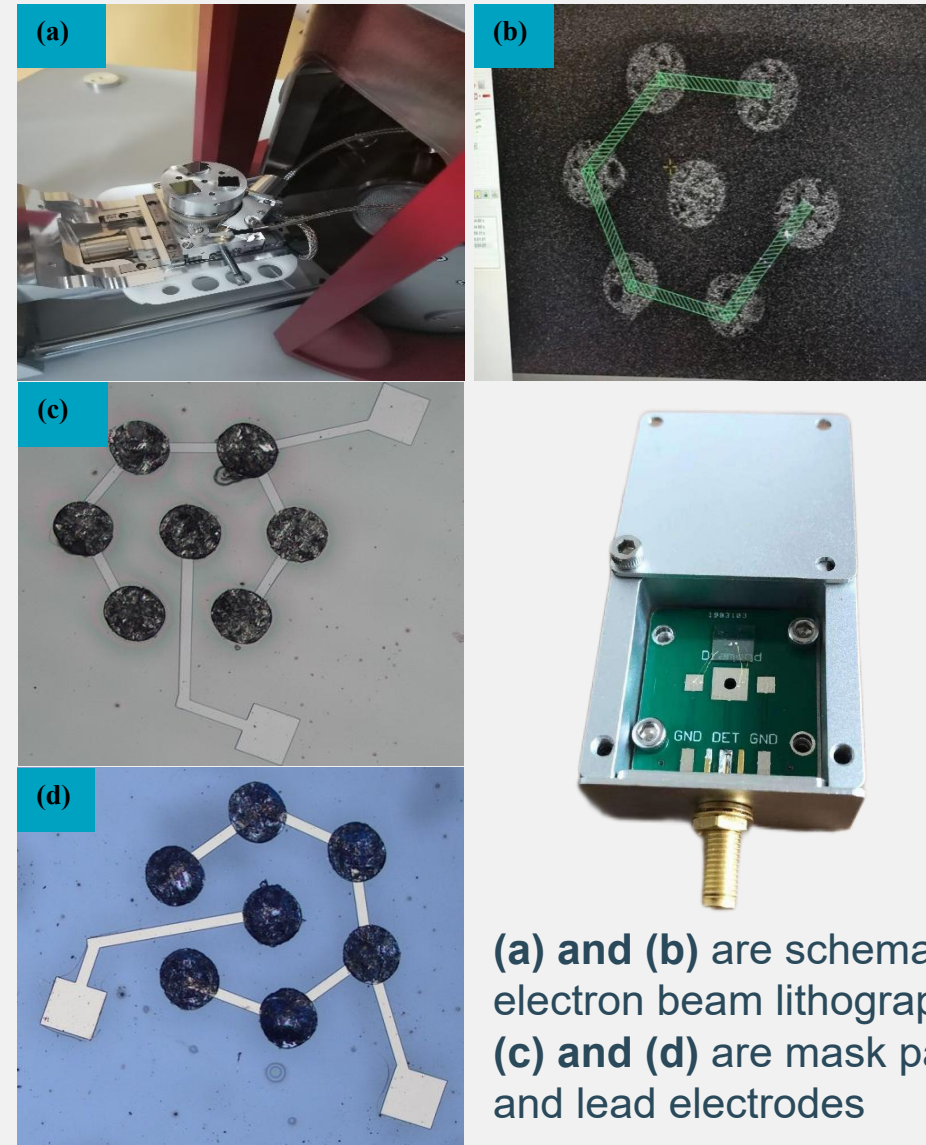


Fig. 7 Image of the filled metal indium electrode



Entrance hole / Exit hole

Fig. 8 Electrode interconnection and packaging



(a) and (b) are schematic of electron beam lithography
(c) and (d) are mask patterns and lead electrodes

Electrical characteristics of 3D SiC structure

Discrete electrode test

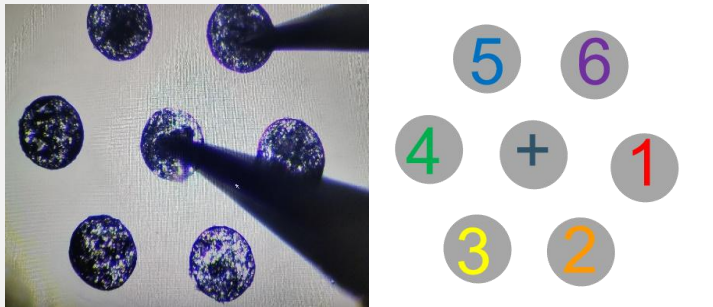


Fig. 9 The test process diagram and electrode number

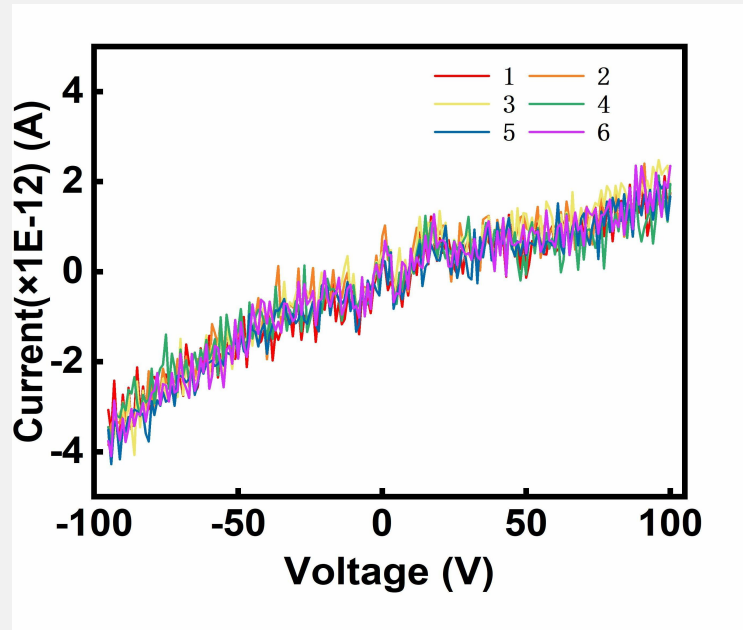


Fig. 10 I-V curve of the discrete electrode device

Interconnection electrode test

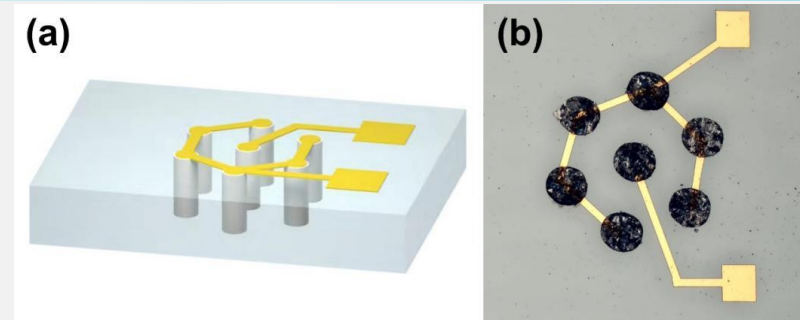


Fig. 11 Schematic of electrode interconnection

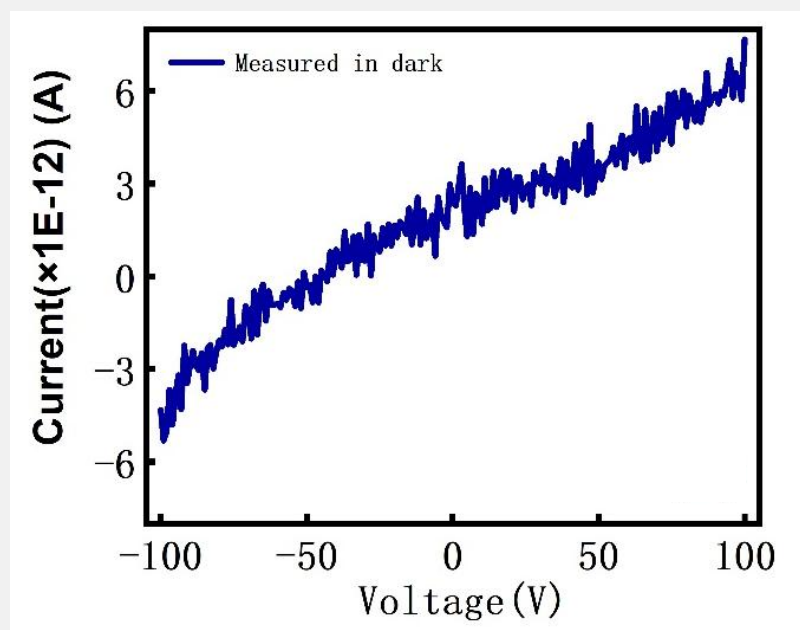
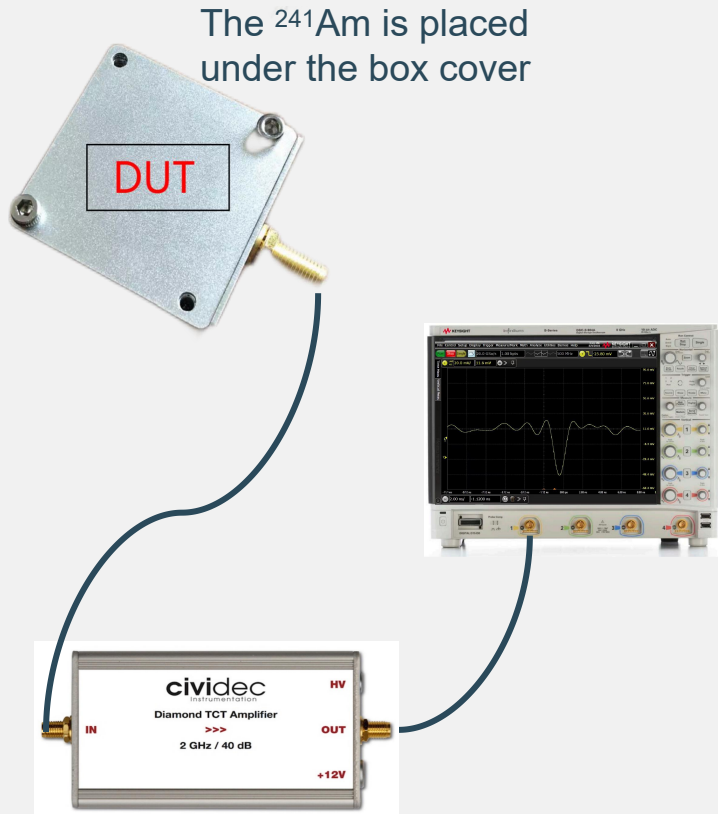


Fig. 12 I-V curve of the interconnection electrode device

Particle response of 3D SiC structure



Cividec TCT BroadBand

Fig. 13 Schematic diagram of test system

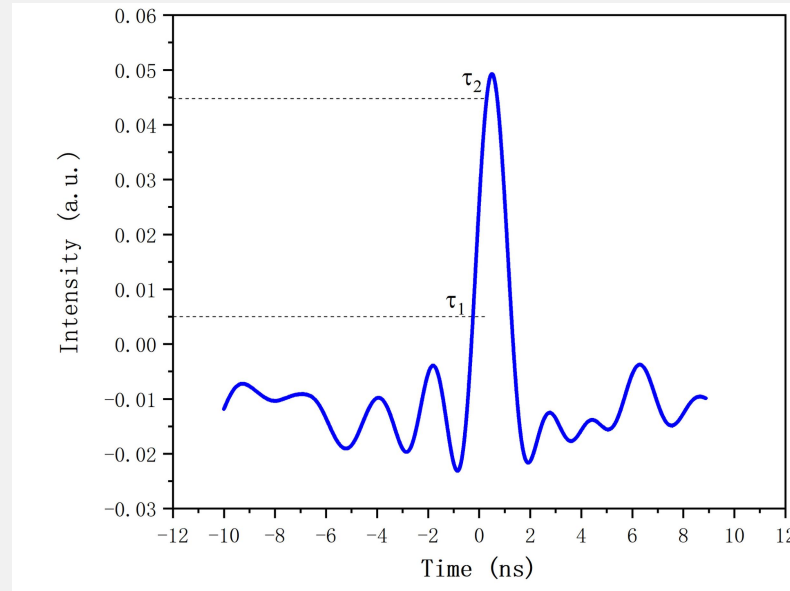


Fig. 14 Alpha particle response result of 3D SiC detector

Signal of 3D-SiC@1V/ μm

The signal rise up from 10% to 90% of the maximum value is 662.75 ps
Entire signal time 1.5 ns

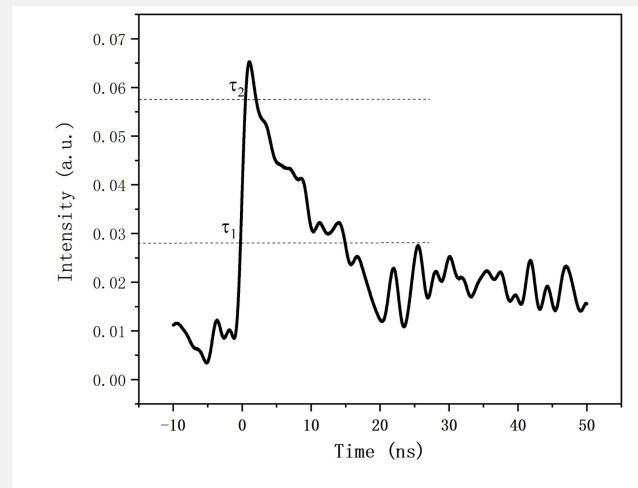


Fig. 15 Alpha particle response result of Schottky devices

Signal of SBD @-60V

The signal rise up from 10% to 90% of the maximum value is 914.06 ps
Entire signal time 15.1 ns

Prospect



- ◆ Making terminal protection structure.
- ◆ Further Study radiation detection performance (Time resolution).
- ◆ Carry out multi-device integration research,

Thanks !